

NMR Chemical Shifts in Hard Carbon Nitride Compounds

Young-Gui Yoon,¹ Bernd G. Pfrommer,¹ Francesco Mauri,² and Steven G. Louie¹

¹Department of Physics, University of California at Berkeley, Berkeley, California 94720

and Materials Sciences Division, Lawrence Berkeley National Laboratory, Berkeley, California 94720

²Institut Romand de Recherche Numérique en Physique des Matériaux (IRRMA), PPH-Ecublens, 1015 Lausanne, Switzerland

(Received 8 December 1997)

We show that NMR chemical shift spectroscopy could help to identify the crystalline phases of hard carbon nitride compounds. To this purpose we compute the NMR chemical shifts of defect zinc-blende, cubic, α -, β -, and graphitic C_3N_4 with a newly developed *ab initio* method. The C shifts can be used to identify the CN bonds and to characterize C hybridization. The N shifts distinguish the α - C_3N_4 from the β - C_3N_4 phases, and indicate the presence of the graphitic phase. [S0031-9007(98)05665-8]

PACS numbers: 76.60.Cq, 71.15.Mb, 82.80.Ch

Carbon nitride compounds have been predicted [1] to exhibit extraordinary hardness, with some structures possibly being harder than diamond [2]. This has stimulated substantial research efforts in search of these materials, employing both experimental [3–14] and theoretical [2,13,15,16] methods.

Shortly after the possibility of high bulk modulus due to the expected short C-N bond lengths was recognized [1], the β - C_3N_4 [2] and later the defect zinc-blende [16], α - C_3N_4 [2], and cubic- C_3N_4 [2] structures were proposed. The theoretical bulk moduli of these structures are 427, 425, 425, and 496 GPa, respectively. Experimental studies, mostly on thin films, followed soon, finding nanometer to micrometer sized crystals embedded usually in an amorphous matrix [3,6,8,11,12]. In several cases [3,6,11] the crystallites were believed to be of the β - C_3N_4 structure, but it has been pointed out later [2] that the α - C_3N_4 structure would comply better with the experimental data. Crystallites with a tetragonal structure [12] and even a monoclinic phase [12] have been reported recently. When using a chemical precursor technique, the defect zinc-blende structure also appears to form [13].

In all experiments, the crystallites obtained are too small to allow a conclusive x-ray diffraction (XRD) analysis. Therefore, structural determinations have been done with XRD in combination with other techniques, e.g., electron diffraction [3,6,8,11–13], x-ray photoelectron spectroscopy [3,8,10], electron energy loss spectroscopy [4], backscattering [3,6,8,10,11,17], and transmission electron microscopy [6,11,12,14]. Still, the determination of the structure of the crystallites remains difficult and not definitive, often because of the obscuring signals from the amorphous matrix or the substrate [11].

In this Letter, we suggest the use of nuclear magnetic resonance (NMR) chemical shift for C-N compound sample characterizations. NMR shift experiments are becoming increasingly popular for characterizing thin-film samples of amorphous carbon [18–23] and silicon [24]. By applying a recently developed *ab initio* method [25], we predict the NMR chemical shifts for C and N atoms of five different low-energy C_3N_4 structures. Our theoretical

data allow an interpretation of experimental NMR spectra, thereby opening a new way for C-N compound characterization. Unlike XRD, NMR experiments do not require long range order, and, as we shall see, should be able to clearly identify the signals from the amorphous sp^2 -bonded matrix, and the crystalline sp^3 -bonded phases. Other phases, such as the defect zinc-blende and cubic C_3N_4 cannot be distinguished by their NMR chemical shift, and other experimental techniques must be invoked. To our knowledge, only two NMR shift experiments on thin amorphous CN_x films have been performed [5,26], which showed the absence of sp^3 bonds, but did not aim at characterizing possible crystalline CN compounds.

Out of the many proposed structures, we pick the five different C_3N_4 candidates shown in Fig. 1 and compute their NMR chemical shifts [27]. The defect zinc-blende cubic structure [16] with space group $P\bar{4}3m$ is examined because of recent experimental findings [13]. We include the predicted low-compressibility cubic structure [2] with symmetry $I\bar{4}3d$, because of the potential technological importance of this hypothetical phase. Finally, we consider β - C_3N_4 [15] and α - C_3N_4 [2] which have likely been observed in experiments. The aforementioned four structures all have C in sp^3 and N in a threefold coordination. That is, each C has four N neighbors and each N has three C neighbors. The fifth structure we study is the graphitic C_3N_4 phase [2], which is actually predicted to be the energetically most favorable form of C_3N_4 . Here, the C atoms are all sp^2 bonded with three N neighbors. Two of the N atoms [1(a) and 1(f) in the Wyckoff site notations] are bonded to three C atoms; the others are in a twofold, bent coordination, with two C neighbors.

In NMR measurements, the chemical shift is one third of the trace of the chemical shift tensor, $\sigma(\mathbf{r}) = \text{Tr}[\vec{\sigma}(\mathbf{r})]/3$, which connects the induced magnetic field to the external uniform applied magnetic field, $\mathbf{B}_{\text{in}}(\mathbf{r}) = -\vec{\sigma}(\mathbf{r})\mathbf{B}_{\text{ext}}$. We compute σ following Ref. [25]. The electronic structure is described using density functional theory in the local density approximation. As the core contributions to σ for C and N are insensitive to the chemical environment [28], we consider the magnetic response

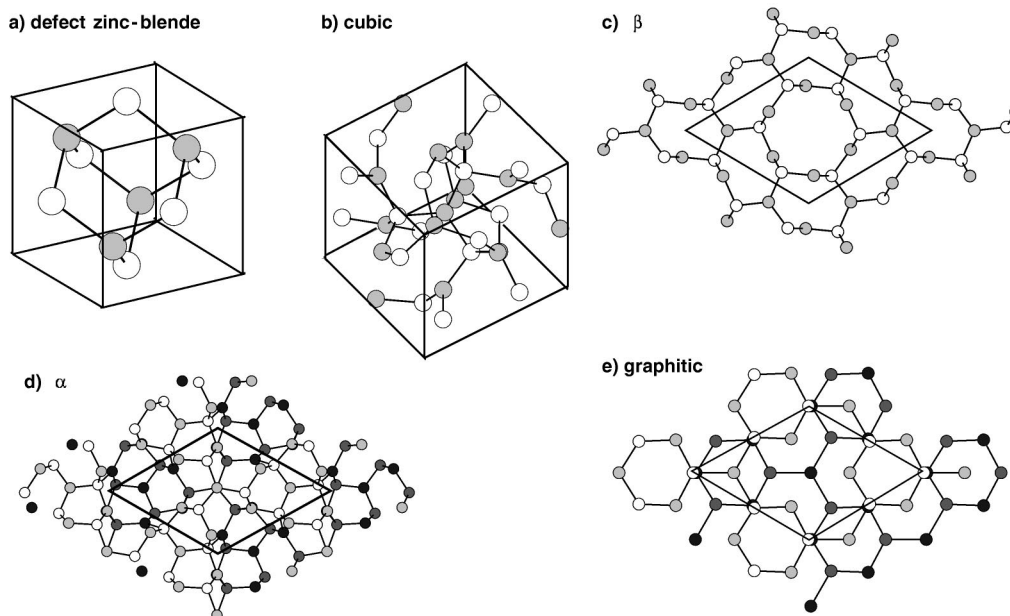


FIG. 1. Ball and stick models of the studied C_3N_4 phases. For the defect zinc-blende (a), cubic (b), and the β phase (c); the C and N atoms are white and grey, respectively. The α structure (d) and the graphitic phase (e) both consist of two layers. The upper layer shows the C atoms in white and the N atoms in light grey. In the lower layer, the C and N atoms are dark grey and black, respectively.

of the valence electrons only. We use norm-conserving pseudopotentials [29] in the Kleinman-Bylander form [30]. For both C and N, nonlocal s projectors augment the local potential. We expand the wave functions in a plane-wave basis set up to an energy cutoff of 100 Ry [31].

Following the experimental convention, we will quote chemical shifts with respect to standard reference systems of a neat liquid sample with spherical shape at 300 K. The C shifts are given with respect to tetramethylsilane (TMS) [32] by $\delta_{TMS}(\text{sample}) = -[\sigma(\text{sample}) - \sigma(\text{TMS})]$, where σ is the absolute chemical shift. For N, nitromethane is used [32] as standard [33]: $\delta_{CH_3NO_2}(\text{sample}) = -[\sigma(\text{sample}) - \sigma(CH_3NO_2)]$.

To test the validity of our pseudopotential approach, and to explore trends in the C shifts, we calculate C δ for a set of small molecules (Table I). In the series of molecules CH_4 , CH_3NH_2 , $CH_2(NH_2)_2$, $CH(NH_2)_3$, and $C(NH_2)_4$, the substitution of hydrogen by amine groups leads to deshielding of the C. A similar effect, but less pronounced, is observed for N in the series NH_3 , CH_3NH_2 , $(CH_3)_2NH$, and $(CH_3)_3N$. In all cases but pyridine, the neighbors of N are sp^3 C, i.e., all C-N bonds are single bonds like those in the hard CN compounds. In these molecules, the agreement between computed and measured shifts is very good. In pyridine (NC_5H_5), since the C are sp^2 hybridized, the N p_z orbital can form an additional resonant π bond with the C p_z orbitals like in the graphitic C_3N_4 phase. The different bonding situation is reflected in much larger C and N δ . The theory reproduces the large increase of δ , but the quantitative agreement with experiment is less satisfactory.

Table II shows the computed C chemical shifts for the five different C_3N_4 phases, along with the coordination number of the C atom. The rightmost column gives the fraction of C atoms in this configuration, which relates to the relative intensity of the NMR signal. Focusing on the shifts of the fourfold coordinated C atoms, we find they

TABLE I. Computed and experimental C and N chemical shifts for selected molecules in the gas phase. Values in parentheses are aligned with experiments [32,33]. Geometries are taken from Ref. [34] (CH_4), Ref. [35] (CH_3NH_2 , N_2H_4), Ref. [36] (NH_3 , pyridine, $(CH_3)_2NH$, $(CH_3)_3N$), and from relaxation within the local density approximation [$CH_2(NH_2)_2$, $CH(NH_2)_3$, $C(NH_2)_4$].

Molecule	C δ_{TMS} [ppm]		N $\delta_{CH_3NO_2}$ [ppm]	
	Theory	Expt.	Theory	Expt.
CH_4	(-11)	-11 ^b		
CH_3NH_2	27	26 ^b	-387	-377 ^{a,c}
$CH_2(NH_2)_2$	52		-347	
$CH(NH_2)_3$	67		-332	
$C(NH_2)_4$	80		-321	
$(CH_3)_2NH$	37		-369	-370 ^{a,c}
$(CH_3)_3N$	45		-362	-363 ^{a,c}
NH_3			(-402)	-402 ^d
N_2H_4			-340	-335 ^{a,c}
Pyridine (NC_5H_5)	C ₂	132	150 ^{a,e}	-105
	C ₃	108	124	
	C ₄	117	136	

^aExperiments are done on liquid or solution.

^bRef. [38].

^cRef. [41].

^dRef. [39].

^eRef. [42].

^fRef. [34].

TABLE II. Computed C chemical shifts (δ_{TMS}) and coordination number for five different C_3N_4 structures. The second column indicates the Wyckoff site of the atoms.

C_3N_4 phase	Sites	$\text{C } \delta_{\text{TMS}}$		
		Theory [ppm]	Coord.	Fraction ^a
Defect zinc-blende ^b	3(<i>c</i>)	93	4	1
Cubic ^c	12(<i>b</i>)	91	4	1
β^b	6(<i>h</i>)	82	4	1
α^c	6(<i>c</i>)	86	4	1/2
	6(<i>c</i>)	86	4	1/2
Graphitic ^b	3(<i>j</i>)	144	3	1/2
	3(<i>k</i>)	144	3	1/2

^aFraction of corresponding C atoms.

^bCoordinates are taken from Ref. [16].

^cCoordinates are from Ref. [2]; the two different 6(*c*) sites are labeled C(1) and C(2) in Ref. [2].

all fall within a fairly narrow range of about 80 to 90 ppm. This value is markedly different from fourfold coordinated diamond, which has a shift of 36 ppm (theory [23]) or 34.5 ppm (experiment [42]), but is close to the 80 ppm obtained for $\text{C}(\text{NH}_2)_4$ (Table I). A general trend can be observed for molecules with a tetrahedrally configured C atom, but varying ligands. For instance, in the series CH_4 , CCl_4 , and CF_4 , the $\text{C } \delta_{\text{TMS}}$ is -11.0 , 96.7 , and 123.6 ppm, respectively, increasing with electronegativity [28].

Given the limited resolution of solid-state NMR experiments, it will be difficult to distinguish the first four phases from each other by looking at the C shifts alone. However, their signal appears between the sp^3 and sp^2 peaks of amorphous C [22] at about 70 and 130 ppm, respectively, and should be detectable if a sufficient fraction of the sample consists of such C_3N_4 compounds. For the graphitic C_3N_4 phase, we predict a carbon shift of 144 ppm. This larger shift is typical of sp^2 hybridized C.

In Table III we present the calculated N shifts of the C_3N_4 solids. Similar to the C shifts, we observe a large

TABLE III. Computed N chemical shifts ($\delta_{\text{CH}_3\text{NO}_2}$) and coordination number for five different C_3N_4 structures. The second column indicates the Wyckoff site of the atoms.

C_3N_4 phase	Sites	$\text{N } \delta_{\text{CH}_3\text{NO}_2}$		
		Theory [ppm]	Coord.	Fraction ^a
Defect zinc-blende ^b	4(<i>e</i>)	-314	3	1
Cubic ^c	16(<i>c</i>)	-317	3	1
β^b	2(<i>c</i>)	-314	3	1/4
	6(<i>h</i>)	-311	3	3/4
α^c	2(<i>a</i>)	-335	3	1/8
	2(<i>b</i>)	-258	3	1/8
	6(<i>c</i>)	-307	3	3/8
	6(<i>c</i>)	-313	3	3/8
Graphitic ^c	1(<i>a</i>)	-240	3	1/8
	1(<i>f</i>)	-241	3	1/8
	3(<i>k</i>)	-168	2	3/8
	3(<i>j</i>)	-164	2	3/8

^aFraction of corresponding N atoms.

^bCoordinates are taken from Ref. [16].

^cCoordinates are from Ref. [2]; the two different 6(*c*) sites are labeled N(3) and N(4) in Ref. [2].

difference between the graphitic phase and the other C_3N_4 structures. This is not unexpected, since the N at 3(*k*) and 3(*j*) positions of the graphitic phase are twofold coordinated unlike in any other compound, and all the N have their C nearest neighbors in sp^2 rather than sp^3 configuration. This allows resonant π bonds between the N and its C neighbors. Equally important is the fact that the positions and the number of N peaks in $\alpha\text{-C}_3\text{N}_4$ are clearly different from those of the other C_3N_4 phases. This should allow one to resolve the question whether $\alpha\text{-C}_3\text{N}_4$ or $\beta\text{-C}_3\text{N}_4$ is observed in experiment [2]. However, neither the C nor the N shift is sufficient to distinguish the cubic and the defect zinc-blende C_3N_4 .

The variation of the N shift in $\alpha\text{-C}_3\text{N}_4$ by about 75 ppm is surprising at first, since they are all threefold coordinated, and the bond lengths range only from 1.41 to 1.50 Å. Similarly, the calculated value for pyridine is -105 ppm (see Table I), which is 61 ppm shifted from the graphitic phase -166 ppm, although the coordination and geometry are comparable. Other researchers had noticed the extraordinary sensitivity of N shifts to their environment before. For example, in Ref. [28] the difference between the *cis* and *trans* isomers of an HNNH molecule is ~ 100 ppm. This sensitivity has been attributed to the strong influence of the lone pair electrons [28]. In short, N shifts are difficult to determine from the geometry or from a comparison with molecular systems.

Notice that, in the experimental spectra on amorphous CN_x [26], a peak at -105 ppm is found [43], which is not too far from the averaged -166 ppm shift we find for the twofold coordinated N in the graphitic C_3N_4 phase. However, the lack of a peak near -240 ppm from the threefold coordinated N indicates the absence of graphitic C_3N_4 in this experiment.

Finally, for completeness, we quote our calculated bulk magnetic susceptibilities (in $\text{ppm cm}^3/\text{mol}$) which are -27 (defect zinc-blende), -29 (cubic), -37 ($\alpha\text{-C}_3\text{N}_4$), -34 ($\beta\text{-C}_3\text{N}_4$), and -37.5 (graphitic C_3N_4).

In summary, our calculations demonstrate that NMR chemical shift experiments may be used to characterize the C_3N_4 compounds. The observed C shift should be clearly distinguishable from the amorphous C signal. The N shifts can be used to discern the α - and $\beta\text{-C}_3\text{N}_4$ phases.

This work was supported by the NSF under Grant No. DMR-9520554, by the Office of Energy Research, Office of Basic Energy Sciences, Materials Sciences Division of the U.S. Department of Energy under Contract No. DE-AC03-76SF00098, and by the Swiss NSF under Grant No. 20-49486.96. Computer time was provided by the NSF at the National Center for Supercomputing Applications and by the DOE at the Lawrence Berkeley National Laboratory's NERSC center.

[1] M. L. Cohen, Phys. Rev. B **32**, 7988 (1985).

[2] D. Teter and R. J. Hemley, Science **271**, 53 (1996).

- [3] C. Niu, Y.Z. Lu, and C.M. Lieber, *Science* **261**, 334 (1993).
- [4] T.H. Sekine *et al.*, *J. Mater. Sci. Lett.* **9**, 1376 (1990).
- [5] L. Maya, D.R. Cole, and E.W. Hagaman, *J. Am. Ceram. Soc.* **7**, 1686 (1991).
- [6] J. Rivière *et al.*, *Mater. Lett.* **22**, 115 (1995).
- [7] J. Cuomo *et al.*, *J. Vac. Sci. Technol.* **16**, 299 (1979).
- [8] Z.-M. Ren *et al.*, *Phys. Rev. B* **51**, 5274 (1995).
- [9] H.-X. Han and B.J. Feldman, *Solid State Commun.* **65**, 921 (1988).
- [10] D. Marton *et al.*, *Phys. Rev. Lett.* **73**, 118 (1994).
- [11] K.M. Yu *et al.*, *Phys. Rev. B* **49**, 5034 (1994).
- [12] L.P. Guo *et al.*, *Chem. Phys. Lett.* **268**, 26 (1997).
- [13] J. Martin-Gil *et al.*, *J. Appl. Phys.* **81**, 2555 (1997).
- [14] Y. Chen, L. Guo, and E. Wang, *Philos. Mag. Lett.* **75**, 155 (1997).
- [15] A.Y. Liu and M.L. Cohen, *Phys. Rev. B* **41**, 10727 (1990).
- [16] A.Y. Liu and R.M. Wentzcovitch, *Phys. Rev. B* **50**, 10362 (1994).
- [17] Z.J. Zhang, S. Fan, and C.M. Lieber, *Appl. Phys. Lett.* **26**, 3582 (1995).
- [18] S. Kaplan, F. Jansen, and M. Machonkin, *Appl. Phys. Lett.* **47**, 750 (1985).
- [19] R.H. Jarman, G.J. Ray, R.W. Standley, and G.W. Zajac, *Appl. Phys. Lett.* **49**, 1065 (1986).
- [20] M.A. Tamor, W.C. Vassell, and K.R. Carduner, *Appl. Phys. Lett.* **58**, 592 (1991).
- [21] A. Grill and V. Patel, *Appl. Phys. Lett.* **60**, 2089 (1992).
- [22] C. Jäger, J. Gottwald, H.W. Spiess, and R.J. Newport, *Phys. Rev. B* **50**, 846 (1994).
- [23] F. Mauri, B.G. Pfommer, and S.G. Louie, *Phys. Rev. Lett.* **79**, 2340 (1997).
- [24] Y. Wu *et al.*, *Phys. Rev. Lett.* **77**, 2049 (1996).
- [25] F. Mauri, B. G. Pfrommer, and S.G. Louie, *Phys. Rev. Lett.* **77**, 5300 (1996).
- [26] D. Li *et al.*, *J. Vac. Sci. Technol. A* **12**, 1470 (1994).
- [27] Other interesting candidate structures include the monoclinic and tetragonal phases reported in [12]. We did not compute their chemical shifts because there is no theoretical prediction of the exact structure or stoichiometry.
- [28] W. Kutzelnigg, U. Fleischer, and M. Schindler, in *NMR Basic Principles and Progress*, edited by P. Diehl (Springer-Verlag, New York, 1990), No. 23, pp. 167–253.
- [29] N. Troullier and J.L. Martins, *Phys. Rev. B* **43**, 1993 (1991).
- [30] L. Kleinman and D.M. Bylander, *Phys. Rev. Lett.* **48**, 1425 (1982).
- [31] NMR chemical shift calculations require higher quality wave functions than total energy calculations. Henceforth, we use pseudopotentials with smaller cutoff radii and plane-wave basis with a higher energy cutoff.
- [32] We do not directly compute $\sigma(\text{TMS})$ and $\sigma(\text{CH}_3\text{NO}_2)$; for the C δ_{TMS} , we fix $\sigma(\text{TMS})$ by imposing that the computed value of δ_{TMS} for gas CH_4 is equal to the experimental value of -11 ppm [37]; for the $\delta_{\text{CH}_3\text{NO}_2}$, we fix $\sigma(\text{CH}_3\text{NO}_2)$ by imposing that the computed value of $\delta_{\text{CH}_3\text{NO}_2}$ for gas NH_3 is equal to the experimental value of -402 ppm [33].
- [33] $\delta_{\text{CH}_3\text{NO}_2}$ for gas NH_3 is obtained as the sum of a shift of -326.16 ppm between the NH_3 and the N_2 isolated molecules [39], a -74.7 ppm shift between the isolated N_2 molecule and liquid CH_3NO_2 in a cylindrical sample perpendicular to the magnetic field [39], and finally a -0.82 ppm correction to a spherical sample shape.
- [34] A.M.L. Lee, N.C.H. Handy, and S.M. Colwell, *J. Phys. Chem.* **103**, 10095 (1995).
- [35] M. Dickson and A. Becke, *J. Phys. Chem.* **99**, 3898 (1993).
- [36] D.R. Lide, in *CRC Handbook of Chemistry and Physics* (CRC Press, Boca Raton, New York, 1997), 78th ed.
- [37] A.K. Jameson and C.J. Jameson, *Chem. Phys. Lett.* **134**, 461 (1987).
- [38] G. Martin, M. Martin, and J. Gouesnard, in *NMR Basic Principles and Progress*, edited by P. Diehl (Springer-Verlag, New York, 1981), No. 18.
- [39] C.J. Jameson *et al.*, *J. Chem. Phys.* **74**, 81 (1981).
- [40] E. Breitmaier and W. Voelter, *Carbon-13 NMR Spektroskopie* (Verlag Chemie, Weinheim, 1987).
- [41] A.J. DiGioia, G.T. Furst, L. Psota, and R. Lichter, *J. Phys. Chem.* **82**, 1644 (1978).
- [42] L. Merwin, C. Johnson, and W. Weimer, *J. Mater. Res.* **9**, 631 (1994).
- [43] The experimental data is 277 ppm referenced to liquid NH_3 . We convert to the CH_3NO_2 scale following Ref. [39]; $\delta_{\text{CH}_3\text{NO}_2} = \delta_{\text{NH}_3} - 382$ ppm.